Experimental Investigation on Heat Transfer and Pressure Drop Characteristics of Food Additive in Dimple Plate Heat Exchanger

ARUMUGAM GOPAL[1*], PRABHAKARAN DURAISAMY[2],
THIRUMARIMURUGAN MARIMUTHU[2]
[1]Department of Petrochemical Engineering, JCT College of Engineering and Technology, Coimbatore, India
[2]Department of Chemical Engineering, Coimbatore Institute of Technology, Coimbatore, India

Abstract: *The present study attempts to examine the heat transfer and pressure drop aspects of a 11-channel dimple plate heat exchanger with hot water as the hot fluid and sodium benzoate (food preservative) as the cold fluid. The outcome of the mass flow rate of hot and cold fluids on the convective heat transfer coefficient and overall heat transfer coefficient were investigated. Furthermore, the effect of Reynolds number on the pressure drop and the Nusselt number were observed. The experimental results demonstrated that when the mass flow rate of the cold fluid increases, so does the overall heat transfer coefficient and the convective heat transfer coefficient. Convective heat transfer coefficient, overall heat transfer coefficient, pressure drop and Nusselt number were increased when sodium benzoate concentration is varied (0.2, 0.4, 0.6% w/w). A correlation is obtained on the basis of experimental results to estimate the Nusselt number as a function of Reynolds and Prandtl number.*

Keywords: *convective heat transfer coefficient, pressure drop, Reynolds number, food additives*

1.Introduction

Heat exchangers are one of the most significant equipment in chemical and food industries for energy and heat transmission [1]. Among the numerous types of heat exchangers, Plate heat exchanger's (PHE's) possess outstanding heat transfer performance, a compact construction, and the ability to vary the heat transfer area by simply adding or removing plates [2]. Because heat transfer is a major unit action in all industrial processes, optimising heat exchangers is critical to the overall process efficiency. Heat transfer enhancement strategies are several approaches used for increasing heat transfer rate without significantly affecting the overall performance of heat exchanger system. These techniques minimize thermal resistance by enhancing heat transfer surface area or creating turbulence in the fluid flowing through the heat exchanger [3]. Fabricating dimples on the surface of heat source is a viable passive strategy to improve heat exchanger's thermal performance, since the dimples can disrupt the flow of the shear layer and accelerate fluid interblending [4]. To better understand the mechanics and heat transfer changes in a dimple cavity and its surrounding area, early study confined on single dimple impression [5]. Experimental demonstration for the production of an oscillating vortex within the dimple and the occurrence of the vortex can elucidate high heat transmission and low fouling susceptibility of the dimpled surface [6]. Therefore, the use of dimples improves the overall performance of PHE's, according to literature research.

Sodium benzoate is a synthetic chemical commonly used in the food industry, and it is usually considered safe. With a natural *p*H of 4.5, sodium benzoate is a salt of benzoic acid, that is employed as an essential preservative in the food manufacturing against yeast, fungus, and bacteria [7]. The Food and Drug Administration (FDA) has approved sodium benzoate as the first preservative to be used in food products [8]. Despite the multiple applications of sodium benzoate, there is no evidence in the literature supporting the performance analysis of dimpled PHE's using food preservatives.

According to the literature studies, dimpled PHE applications research is confined to single or dual channels using a single plate. Liquids as working fluids have a scarce number of experimental research.

*email: sixface100@gmail.com

The primary objective of this research is to investigate how the flow rate and heat transfer properties affect the Nusselt number of sodium benzoate flowing through an 11-channel dimple plate heat exchanger. Pressure drop, convective heat transfer coefficient, overall heat transfer coefficient, and Nusselt number are all explored as a function of mass flow rate and Reynolds number. Finally, Nusselt number correlation thus obtained are validated using experimental data sets.

2. Materials and methods
2.1. Experimental system
The present study is carried out in a 11-channel single pass dimple plate configuration heat exchanger manufactured by Almech Enterprise, Tamil Nadu, India. The trial set-up is depicted schematically in Figure 1, Table 1 lists the specifications for dimpled PHE. The PHE is configured in Z arrangement i.e, the inlet/exit ports of the two fluids are on either side of the end plates, allowing a counter-flow arrangement for the two fluid streams. Dimple plate heat exchanger is made from stainless steel and thermal conductivity is 36.5 W/m K.
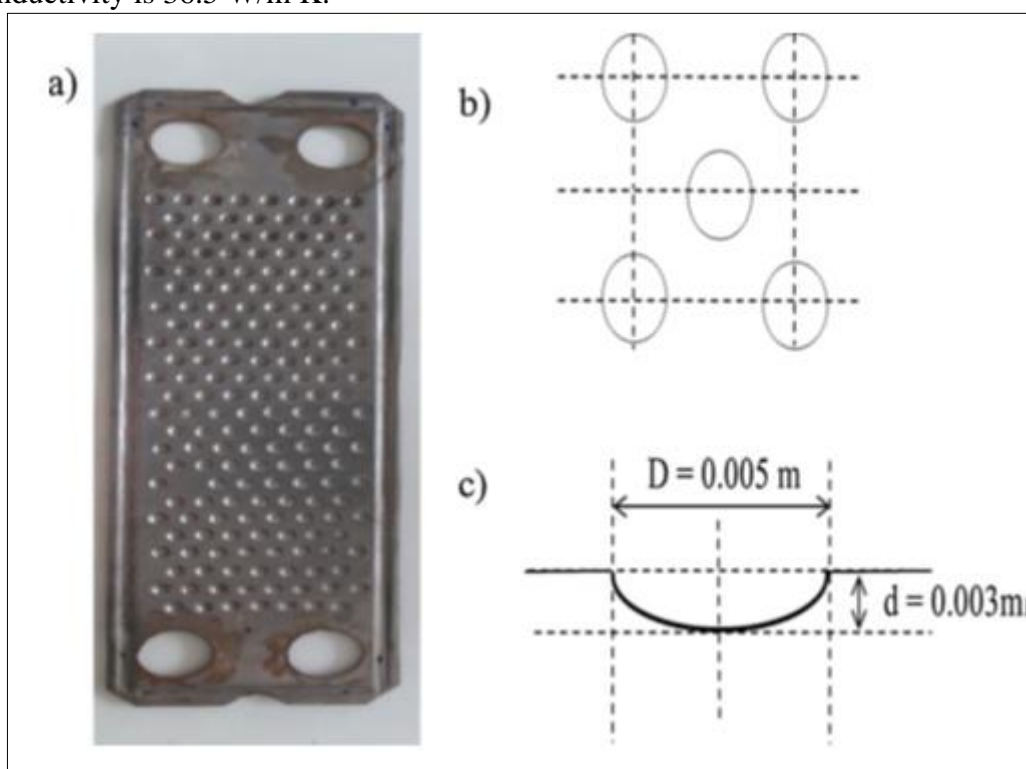
Figure 1. Geometric parameter of apparatus

Table 1. Specification of dimpled PHE

S. No	Particulars	Dimpled PHE
1.	Plate length (l), m	0.28
2.	Plate width (w), m	0.072
3.	Plate channel spacing C_s, m	0.004
4.	Hydraulic diameter (D_h), m	0.00757
5.	Plate thickness (Δx), m	0.0008
6.	Dimple depth (d), m	0.002
7.	Number of plates (N_p)	12
8.	Effective heat transfer area for dimpled PHE (A_p), m^2	0.223

9.	Total number of channels (N_c)	11
10.	Number of cold fluid channel	6
11.	Number of hot fluid channel	5
12.	Pass	Single

The experimental apparatus consists of a cold fluid storage tank, a thermally insulated hot fluid storage tank to prevent heat losses, two stirrers, a pair of 2 KW immersive electric heaters installed inside the hot fluid storage tank, two mono block pumps (0.5 HP), two control valves, a couple of rotameters (0-250 LPH), two U-tube manometers, six PT 100 type thermocouples, a thermostat temperature controller, digital temperature indicator with channel selector, and two separate collecting tanks for storage and recycling the cold and hot fluids.

Table 2. Physical properties of Sodium Benzoate (0.2 % w/w of SB)

S.No	Temperature, (K)	Density, (kg m^{-3})	Viscosity, (Pa .sec) (or) N. sec/m^2	Thermal conductivity, (Wm^{-1} K^{-1})
1	308.15	994.092	0.00157	0.670
2	313.15	990.018	0.00155	0.672
3	318.15	988	0.00152	0.675
4	323.15	985.944	0.00150	0.679
5	328.15	983.915	0.00146	0.681
6	333.15	980.356	0.00143	0.684

Table 3. Physical properties of Sodium Benzoate (0.4 % w/w of SB)

S.No	Temperature, (K)	Density, (kg m^{-3})	Viscosity, (Pa .sec) (or) N. sec/m^2	Thermal conductivity, (Wm^{-1} K^{-1})
1	308.15	990.018	0.001695	0.654
2	313.15	988	0.001675	0.655
3	318.15	985.944	0.00164	0.657
4	323.15	983.9	0.0016	0.659
5	328.15	981.902	0.001575	0.660
6	333.15	979.231	0.00155	0.662

Table 4. Physical properties of Sodium Benzoate (0.6 % w/w of SB)

S.No	Temperature, (K)	Density, (kg m^{-3})	Viscosity, (Pa .sec) (or) N. sec/m^2	Thermal conductivity, (Wm^{-1} K^{-1})
1	308.15	994.092	0.00177	0.618
2	313.15	992.320	0.00175	0.623
3	318.15	990.018	0.001725	0.625
4	323.15	985.944	0.0017	0.628
5	328.15	984.102	0.00167	0.631
6	333.15	981.913	0.001645	0.633

2.2. Experimental procedure

For heat transfer studies, water is utilized as the hot fluid. Various concentrations of sodium benzoate (0.2, 0.4, 0.6% w/w) were dissolved in water and employed as cold fluid. With each 30 L tank, tap water is loaded in the hot liquid storage tank and sodium benzoate in the cold liquid storage tank. Hot fluid temperature is raised by turning on the electric heaters. When the hot fluid reaches the desired temperature, both hot and cold side fluids are circulated between the storage tanks and heat exchanger via mono block pump. Recycling lines transport the two fluids from the exit to separate storage tanks for recycling and reuse. After attaining a steady-state, the entrance and exit temperatures, the flow rate as well as the manometer reading of the two fluids are noted and used for further calculations. The mass flow rate of hot and cold side fluids was continually varied under different flow analysis. Sodium benzoate unadulterated (food grade) was provided by M/s. Merck. For a steady hot liquid mass flow rate and concentration of sodium benzoate, test results were acquired for varied flow rates of sodium

benzoate (0.007 to 0.041 kgs^{-1}). Similarly, trials were evaluated for varied concentrations of sodium benzoate and mass flow rates of hot liquid (0.0136-0.0408 kgs $^{-1}$).

2.3. Data processing

In heat transfer study, the PHE's input and output temperature for hot and cold side fluid is the most important measurement. The studies are carried out with the following assumptions.

1. One-Dimensional incompressible plug flow
2. No significant heat loss and phase change
3. No transmission of heat towards the liquid flow
4. Flawless mixing

The thermal and physical properties of the hot and the cold fluids are determined using the below expressions:

$$T_h = \frac{T_{hi} + T_{ho}}{2} \qquad (1a)$$

$$T_c = \frac{T_{co} + T_{ci}}{2} \qquad (1b)$$

where, T_h − average fluid temperature on the hot side (K)

T_c – average fluid temperature on the cold side (K)

T_{hi}, T_{ho} − denote the hot fluid's steady state temperatures at the entrance and exit (K) respectively.

T_{ci}, T_{co} − denote the cold fluid's steady state temperatures at the entrance and exit (K) respectively.

The thermo physical characteristics of water are referenced [9]. The DSC2A-00837 Differential Scanning Calorimeter was used to detect the specific heat of sodium benzoate solution (0.2, 0.4, 0.6%w/w). The KD2 Pro Thermal Property analyser was utilised to test thermal conductivity, while Brookfield viscometer was used to assess viscosity.

The heat loads of the hot and cold side fluids are represented by the following equations:

$$Q_h = m_h Cp_h [T_{hi} - T_{ho}] \qquad (2a)$$

$$Q_c = m_c Cp_c [T_{co} - T_{ci}] \qquad (2b)$$

where, Q_h, Q_c are the hot and the cold side fluid heat load (W), m_h, m_c and Cp_h, Cp_c denote the mass flow rates (kgs^{-1}) and specific heat capacity ($J\,kg^{-1}K^{-1}$) of hot and cold side fluid.

The following equation (3) is used to get the experimental overall heat transfer coefficient

$$U_{exp} = \frac{Q}{A_p\,\Delta T_{lm}\,F_T} \qquad (3)$$

where, U_{exp} - Experimental overall heat transfer coefficient ($Wm^{-2}\,K^{-1}$)

Q - Average hot and the cold side fluids heat load (W)

A_p - Effective heat transfer area of the plate (m^2)

ΔT_{lm} - Logarithmic mean temperature difference (K) and

F_T - correction factor [10].

$$Q = \frac{Q_h + Q_c}{2} \qquad (3a)$$

$$A_p = (l \times w)(N_c - 1) + (n \times \pi \times d^2) \qquad (3b)$$

where l, w and N_c represent the length (m), width (m) of the plate and the overall channel number in the heat exchanger and n and d denote the dimple number and dimple depth (m). ΔT_{lm} is the

logarithmic mean temperature difference (K) of the counter flow arrangement and F_T is the correction factor.

$$\Delta T_{lm} = \frac{(T_{hi} - T_{co}) - (T_{ho} - T_{ci})}{\ln\frac{(T_{hi} - T_{co})}{(T_{ho} - T_{ci})}} \tag{3c}$$

ΔT_{lm} = Log-mean temperature difference correction factor F_T, is calculated by using the below equation:

$$F_T = \begin{cases} \frac{1}{NTU(1-C^*)} \ln\frac{(1-C^*\varepsilon)}{1-\varepsilon} & \text{if } C^* < 1 \\ \frac{\varepsilon}{NTU-(1-\varepsilon)} & \text{if } C^* > 1 \end{cases} \tag{4}$$

where, C^* - capacity ratio,
ε – Heat exchanger effectiveness
NTU - Number of heat transfer units

$$C^* = \left(\frac{\min(m_c\, cp_c, m_h\, cp_h)}{\max(m_c\, cp_c, m_h\, cp_h)}\right) \tag{4a}$$

$$\varepsilon = \frac{Q}{Q_{max}} \tag{4b}$$

where, $Q_{max} = \min(m_c\, cp_c, m_h\, cp_h)(T_{hi} - T_{ci})$

$$NTU = \frac{U^*\, A_P}{C_{min}} \tag{4c}$$

$$U^* = \frac{Q}{Ap\, \Delta T_{lm}} \tag{4d}$$

U^*- Overall heat transfer coefficient ($Wm^{-2}\, K^{-1}$)

Eq. 5 is used to calculate the individual heat transfer coefficient of respective fluid [11]:

$$\frac{1}{U_{exp}} = \frac{1}{h_c} + \frac{\Delta x}{k_{ss}} + \frac{1}{h_h} \tag{5}$$

where, h_c – Cold fluid's individual heat transfer coefficient ($Wm^{-2}\, K^{-1}$)
h_h – Hot fluid's individual heat transfer coefficient ($Wm^{-2}\, K^{-1}$)
K_{ss} - Plate material thermal conductivity ($Wm^{-1}\, K^{-1}$) and
Δx – Plate thickness (m)

Under same flow analysis, the fluid flow rate is kept the same. Hence, $h_h = h_c = h$ is assumed to be equal for fluid heat transfer coefficient [12]. The individual heat transfer coefficient for same flow of hot and cold side fluids is calculated using the following expression:

$$\frac{1}{h} = \frac{1}{2}\left(\frac{1}{U_{exp}} - \frac{\Delta X}{k_{ss}}\right) \tag{6}$$

$$Nu = \frac{h D_h}{k} \tag{7}$$

where, Nu - Fluid Nusselt number
h - heat transfer coefficient of the fluid ($Wm^{-2}\, K^{-1}$)
D_h - hydraulic diameter (m)
k – Fluid thermal conductivity ($Wm^{-1}\, K^{-1}$).

$$D_h = 4(w \times C_s)/2(w + C_s) \tag{7a}$$

where, w and C_s denote the width (m) and channel spacing (m) of the plate respectively.

The entrance and exit port pressure drop along with the channel pressure drop makeup the overall PHE's pressure drop [13, 14]. The total pressure drop across the dimple PHE can be measured by U-tube manometer using equation 8 stated below:

$$\Delta P_T = \Delta P_{ch} + \Delta P_p = \Delta h(\rho_{Hg} - \rho) g \tag{8}$$

where, ΔP_T - Total pressure drop over the PHE (Pa)

ΔP_{ch} - Channel pressure drop over the PHE (Pa)

ΔP_p - Pressure drop across the ports (Pa)

Δh - The difference between the pressure heads (m)

ρ_{Hg} and ρ - Mercury and the working fluid density (kg m^{-3})

g - acceleration due to gravity (m s^{-2}).

The pressure drop at the entrance and exit ports can be computed with Eq. (8a) [15].

$$\Delta P_P = \frac{1.4\rho u_p^2}{2} \tag{8a}$$

where, u_p - mean fluid velocity (m s^{-1})

ρ - Working fluid density (kg m^{-3})

The pressure drop in the channels can be computed as follows:

$$\Delta P_{ch} = \frac{fl\rho u^2}{2D_h} \tag{8b}$$

where, f - friction factor,

l - Plate length (m),

u - mean fluid velocity in the channel (m s^{-1})

D_h - Mean hydraulic diameter (m)

ρ - Working fluid density (kg m^{-3})

3.Results and discussions

In this experiment, a 11-channel dimpled plate heat exchanger with sodium benzoate as the working fluid was employed. Based on the experimental findings, the effects of hot and cold side fluid concentrations as well as flow rates on Nusselt number were investigated and described below.

3.1. Effect of hot and cold fluid mass flow rates on the overall heat transfer coefficient

The hot and cold fluid's mass flow rate with varying concentrations (0.2, 0.4, 0.6 %w/w) of the cold side fluid is shown in Figure 2a, b, c to demonstrate how the overall heat transfer coefficient is impacted by the cold and hot fluid's mass flow rate. The overall heat transfer coefficient rises when the cold fluid mass flow rate increases from 0.007 to 0.041 kgs^{-1} while the hot fluid mass flow rate remains constant, as shown in Figure 2 a, b, c for a specific concentration of cold fluid (sodium benzoate). Overall heat transfer coefficient changes for concentration variation of 0.2, 0.4, and 0.6 %w/w of cold side fluid are 133.950 - 1099.221 Wm^{-2}K^{-1}, 156.820 - 1211.397 Wm^{-2}K^{-1} and 227.535 - 1271.131 Wm^{-2}K^{-1}, respectively. The findings reveal that when cold fluid mass flow rate increases, so does the overall heat transfer coefficient. This rise is related to a decrease in logarithmic temperature difference, an increase in heat transfer rate owing to rise in temperature difference between fluids, and the development of a secondary flow inside the flow route. Furthermore, when the mass flow rate of cold side fluid rises between 0.007 to 0.041 kgs^{-1} at higher hot fluid flow rates, more secondary vortices occur, resulting in significant variations of the overall heat transfer coefficient. Muthamizhi and Kalaichelvi achieved similar results in their investigation of carboxy methyl cellulose heat transfer properties in plate type heat exchangers [13].
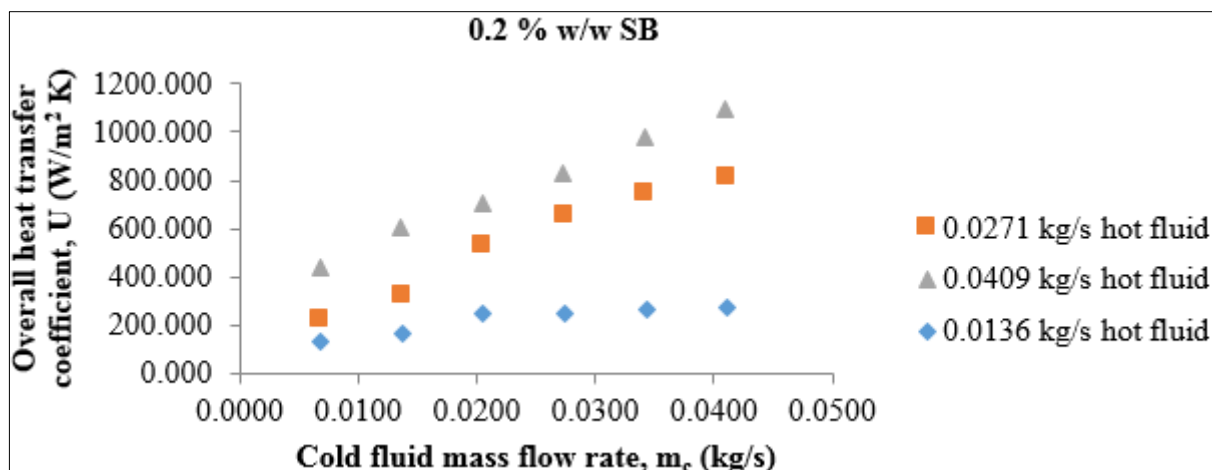
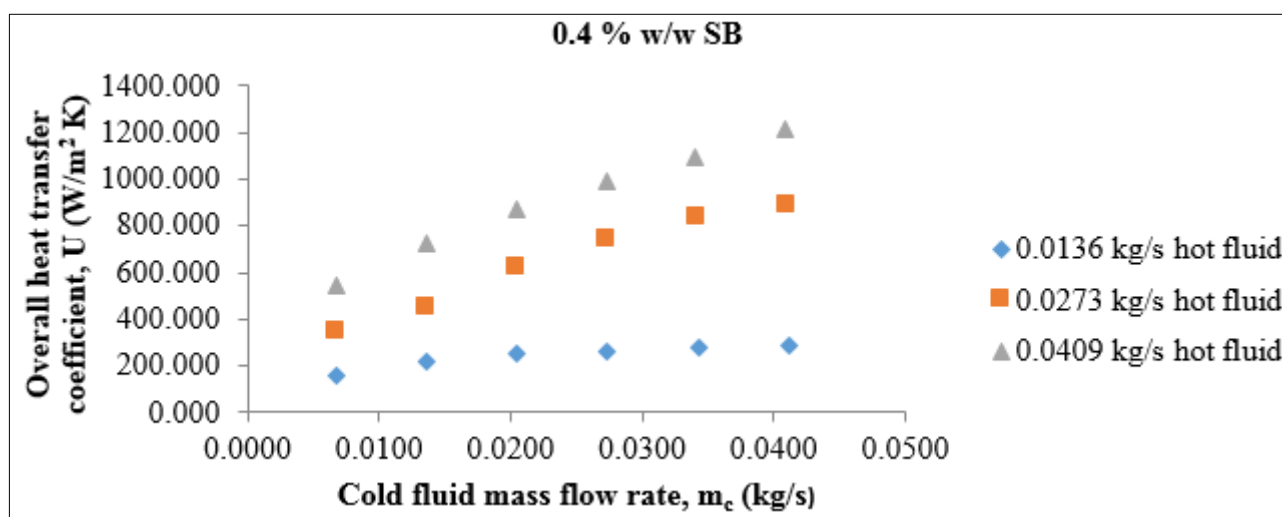**Figure 2a.** The effect of hot and cold fluid mass flow rate on the overall heat transfer coefficient of 0.2 %w/w SB

Figure 2b. The effect of hot and cold fluid mass flow rate on the overall heat transfer coefficient of 0.4 %w/w SB
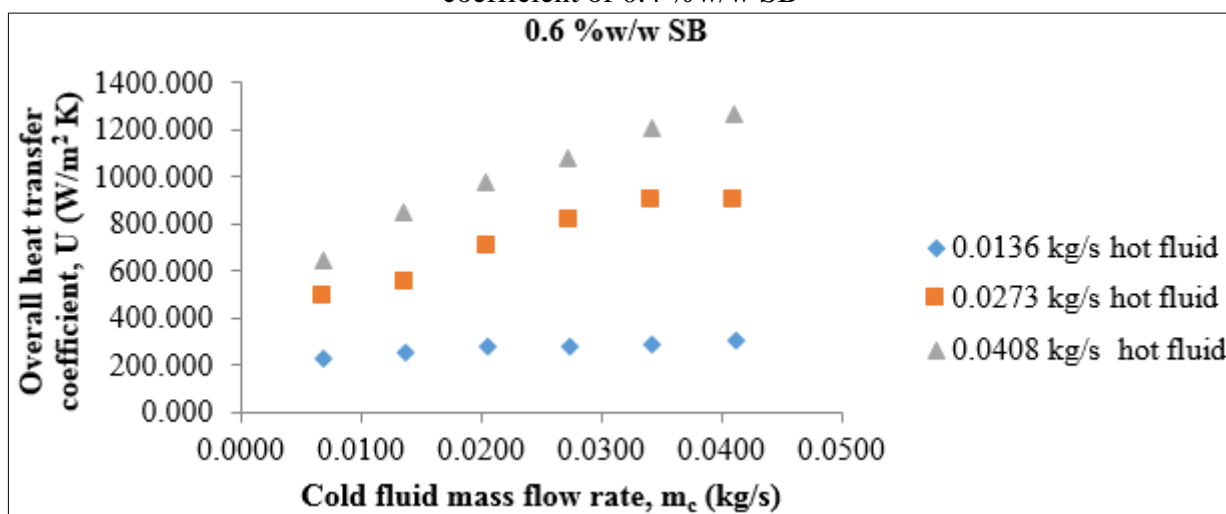

Figure 2c. The effect of hot and cold fluid mass flow rate on the overall heat transfer coefficient of 0.6 %w/w SB

3.2. Heat transfer empirical correlation

Under heat transfer for single-phase condition, the empirical correlation that relates Nusselt number to Reynolds and Prandtl number is given by equation 9.

$$Nu = C \, Re^a \, Pr^b \tag{9}$$

where a, b, and C – exponents and empirical correlation coefficients based on plate patterns and geometrics

Re - Reynolds number
Pr - Prandtl number
Nu- Nusselt number

The experimental exponents and coefficient data such as a, b and C can be calculated using linear regression analysis (LINEST method) [14]. In most associations, the Prandtl number coefficient ranges between 0.33 and 0.4 [15]. Equations 9a and 9b define Re and Pr of fluid as,

$$Re = \frac{\rho v D_H}{\mu} \tag{9a}$$

where ρ - working fluid density (kgm^{-3}),
v - working fluid velocity (ms^{-1}),
D_H - hydraulic diameter (m) and
μ - working fluid viscosity (Pa s)

$$Pr = \frac{C_P \mu}{k} \tag{9b}$$

where Pr - Prandtl number,
C_p - working fluid's specific heat capacity ($J\,kg^{-1}K^{-1}$),
μ - working fluid viscosity (Pa s)
k - working fluid thermal conductivity ($W\,m^{-1}K^{-1}$)

The value of b is taken as 0.33 (for hot fluid) in this correlation. The fluid mass flow rate varies on either plate sides during different flow analysis, therefore U can be estimated by equation 4d, Nu_h is calculated using equation 8, h_h is calculated using equation 7 and lastly h_c is calculated using equation 5. Equation 7 calculates the cold fluid Nusselt number, then the empirical correlation for the single-phase heat transfer of hot fluid developed for same flow analysis is shown in equation 10 below:

$$Nu_h = 0.000014 \, Re^{2.451} \, Pr^{0.33} \tag{10}$$

The heat transfer coefficient of the hot side fluid is estimated using the aforementioned empirical correlation stated in equation 10, and the heat transfer coefficient of the cold side fluid is determined using equation 5. The cold fluid's Nusselt number is then computed using equation 7. Finally, for different amounts of cold fluid, an empirical correlation of the Nusselt number is developed, as shown below

$$Nu_c = 0.195 \, Re^{0.754} \, Pr^{0.4} \tag{11}$$

3.3. Effect of hot and cold fluid mass flow rates on convective heat transfer coefficient

When the hot fluid mass flow rate is held constant, the convective heat transfer coefficient of the cold fluid increases with a rise in the cold fluid mass flow rate from 0.007 to 0.041 kgs^{-1}, as shown in Figure 3a, b, c. Consequently, the convective heat transfer coefficient of the cold fluid increases with a rise in the hot fluid mass flow rate from 0.0136 - 0.0408 kgs $^{-1}$. For 0.2, 0.4, and 0.6 % w/w concentrations of cold fluid, the convective heat transfer coefficients vary from 169.624 to 1352.365 Wm^{-2}K^{-1}, 207.894 to 1504.241 Wm^{-2}K^{-1}, and 353.567 to 1587.309 Wm^{-2}K^{-1}. The increase in cold fluid's convective heat transfer coefficient against mass flow rate is due to the rise in heat transfer rate, Reynolds number, and

secondary flow production, all of which enhances the heat transfer coefficient. Soman et al. discovered similar results trends for the study of Al_2O_3/water nanoparticle in dimpled plate heat exchanger [16].
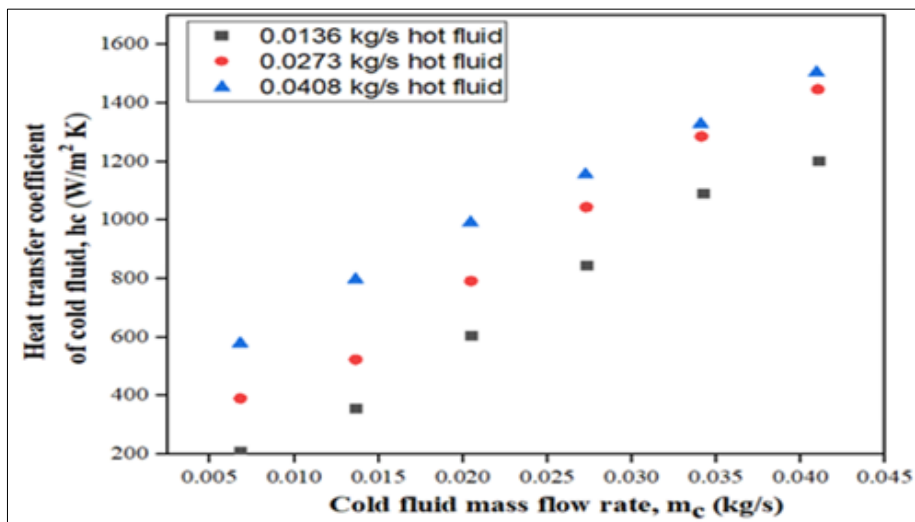
Figure 3a. Effect of mass flow rate of hot and cold fluid on heat transfer coefficient of 0.2% w/w SB, cold fluid
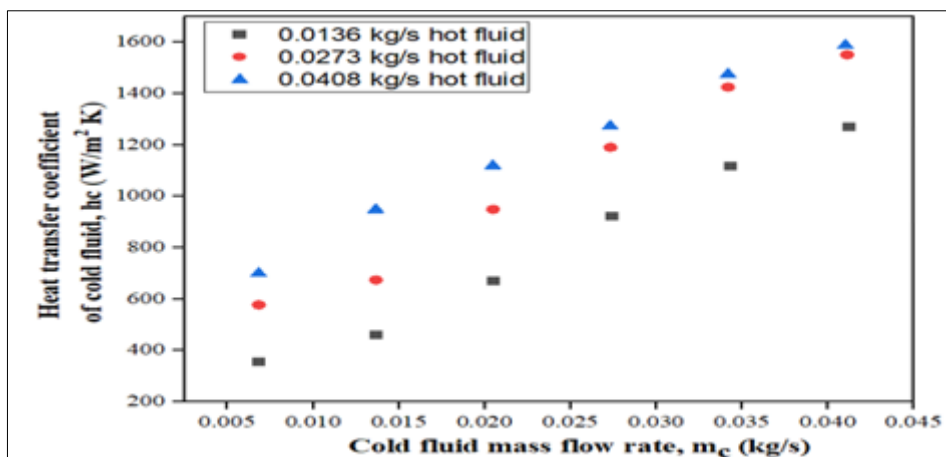
Figure 3b. Effect of mass flow rate of hot and cold fluid on heat transfer coefficient of 0.4% w/w SB, cold fluid
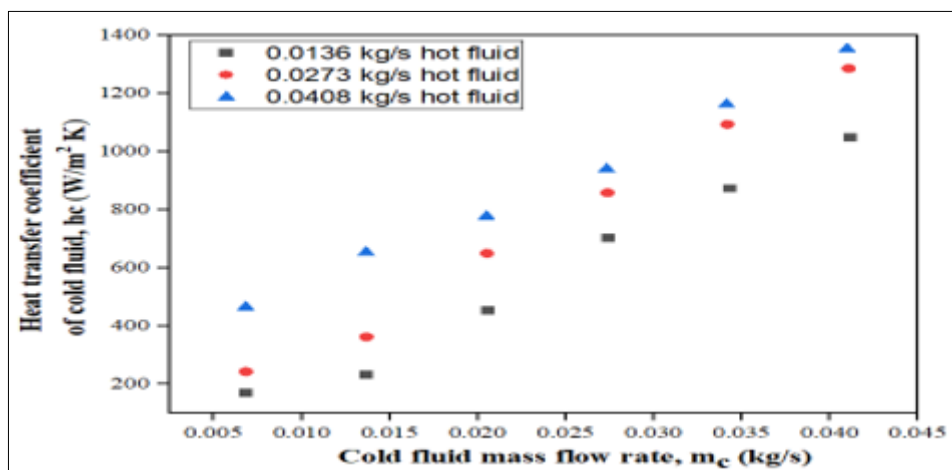
Figure 3c. Effect of mass flow rate of hot and cold fluid on heat transfer coefficient of 0.6% w/w SB, cold fluid

3.4. Impact of Reynolds number on pressure drop

Pressure drop for hot and varied concentrations of cold fluids increases when the Reynolds number of hot and cold side fluids increases with a rise in the mass flow rate of fluid from 0.007 to 0.041 kgs^{-1}, as shown in Figure 4. Pure water and water with 0.2, 0.4, and 0.6 %w/w concentrations of the cold fluid had pressure drop variations of 266.832 - 2668.320 Pa, 2227.748 - 4826.985 Pa, 2599.702 - 5322.518 Pa, 3094.27 - 5940.474 Pa, respectively. The highest-pressure drop is provided by 0.6 %w/w cold fluid, while the minimum is provided by water. A rise in the pressure drop is caused by an increase in the Re, concentration, secondary vortices along with a reduction in viscosity and fluid density while increasing the temperature. Different types of heat exchangers provide similar outcomes. Changing the Re from 100 to 450, raises the pressure drop from 0.3 to 7 kPa for the plate heat exchanger [17]. For a brazed plate heat exchanger with Re varying between 280 to 310, the pressure drop for a water-Al$_2$O$_3$ nanofluid system is found to be in the range of 0.5 to 2.5 kPa [18].
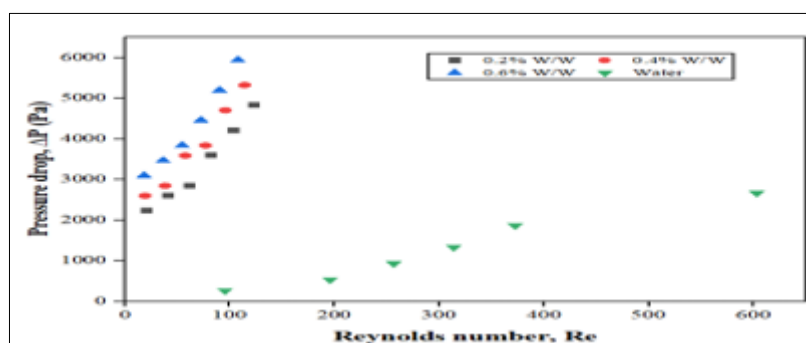

Figure 4. Pressure drop as a function of Reynolds number

3.5. Impact of Reynolds number on Nusselt number

The change in Nusselt number versus Reynolds number for varied concentrations of cold fluid at a steady flow rate of hot fluid at 0.014, 0.027, and 0.041 kgs^{-1} is shown in Figure 5a, b, c. This implies that the Nusselt number rises in parallel with the Reynolds number and the cold fluid concentration. This is attributed to the dimples in the PHE which create a secondary flow within the fluid's flow path [16]. The Nu of the fluids rises while the heat transfer coefficient increases. The Nu is low when the cold side fluid mass flow rate is low, and it is large when the flow rate is high, as depicted in Figure 5a, b, c. This rise in mass flow rate can be attributed towards the creation of turbulence along fluid flow path, which results in a larger Nu value at higher mass flow rates [19].
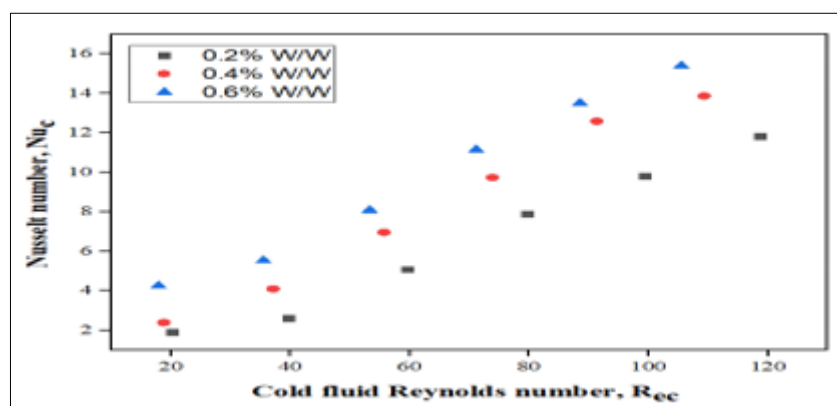

Figure 5a. Effect of Reynolds number on Nusselt number of cold
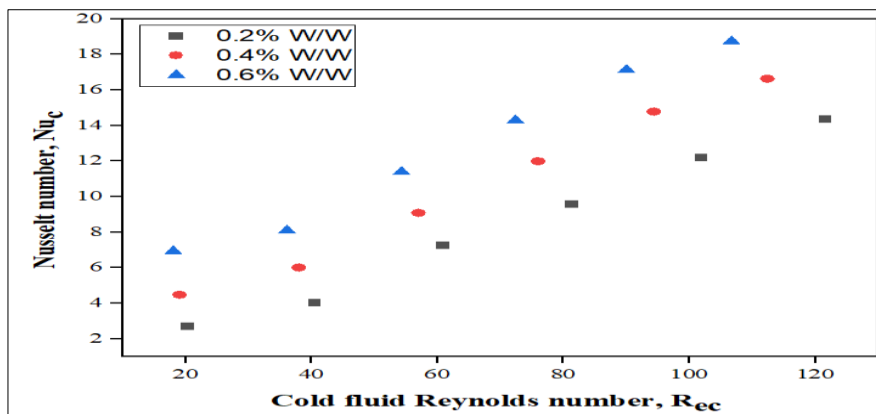fluid for 0.014 kgs^{-1} mass flow rate of hot fluid

Figure 5b. Effect of Reynolds number on Nusselt number of cold
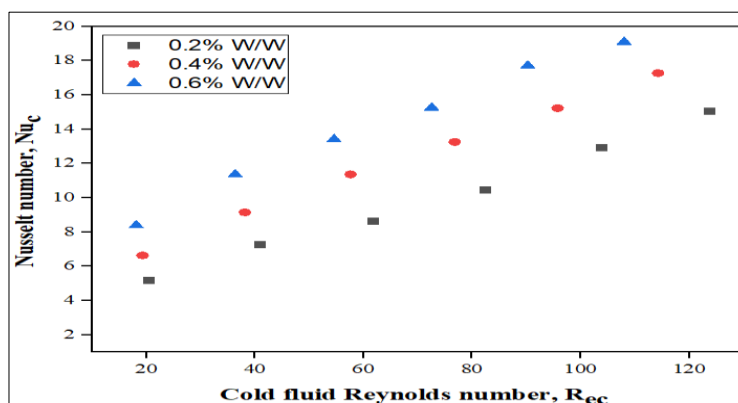fluid for 0.027 kgs^{-1} mass flow rate of hot fluid

Figure 5c. Effect of Reynolds number on Nusselt number of cold
fluid for 0.041 kgs^{-1} mass flow rate of hot fluid

3.6. Comparison of experimental Nu_c number data against Nu_c correlation developed in the present study

Figure 6 compares the experimental Nu_c number data with the Nu_c number correlation obtained by the present study. The hypothesised Nu correlation shows good agreement with the experimental Nu_c number data, as seen in the figure. The Root Mean Square (RMS) discrepancy seen between experimental Nu_c data against the Nu_c number obtained by the proposed correlation is 16.28, with the RMS deviation ranging between +20% and -20%.
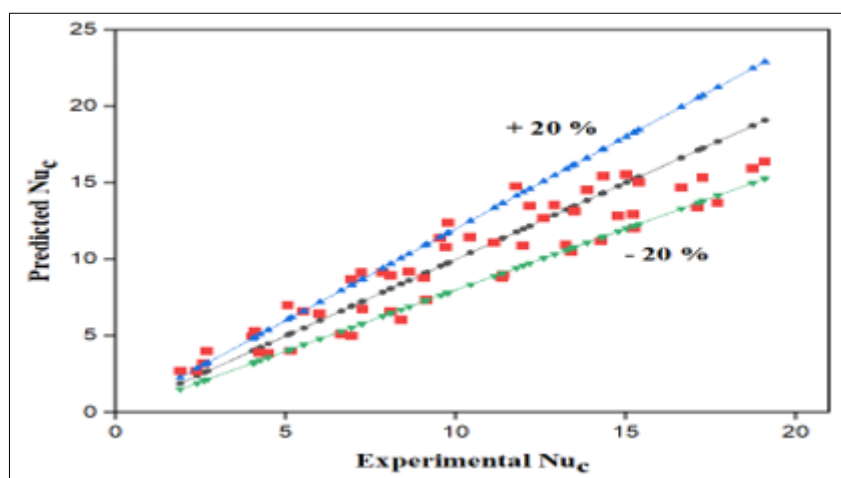

Figure 6. Experimental Nu_c versus predicted Nu_c

4. Conclusions

The heat transfer and pressure drop characteristics of varied concentrations of sodium benzoate working fluid were investigated experimentally using a dimpled plate heat exchanger in this study. The influence of hot and cold side fluids flow rate on the heat transfer coefficient of varying cold fluid concentrations is investigated, and it has been discovered that when the heat transfer coefficient rises as the mass flow rate of both fluid increases. When the cold fluid concentration is increased between (0.2, 0.4, 0.6%w/w), the heat transfer coefficient rises as well. Pressure drops of hot and cold side fluids increase as the Reynolds number rises, according to pressure drop research. An empirical correlation for the Nusselt number of the cold fluid is developed based on the experimental data, and it correlates well with the experimental results within the range of +/-20% for the cold fluid. With an RMS variation of 16.28, the derived empirical relation for the cold fluid's Nusselt number is utilised to forecast the Nusselt number of the specified dimpled Plate heat exchanger. The accuracy of the identified correlation might be enhanced by using a larger set of data points and a broader variety of Reynolds number.

References

1. FARAJOLLAHI, B., S.G. ETEMAD, M. HOJJAT, Heat transfer of nanofluids in a shell and tube heat exchanger, *International Journal of Heat and Mass Transfer,* 53 (2010), 1-3, p. 12-17
2. KUMAR, V., A.K. TIWARI, S.K. GHOSH, Characterization and performance of nanofluids in plate heat exchanger, *Materials Today: Proceedings*, 4 (2017) 2, p. 4070-4078
3. MARADIYA, C., J. VADHER, R. AGARWAL, The heat transfer enhancement techniques and their thermal performance factor, *Beni-Suef University Journal of Basic and Applied Sciences*, 7 (2018) 1, p. 1-21
4. CHEN, Y., Z. LIU, D. HE, Numerical study on enhanced heat transfer and flow characteristics of supercritical methane in a square mini-channel with dimple array, *International Journal of Heat and Mass Transfer*, 158 (2020), p. 119729
5. CHOI, S.M., et al., Heat transfer from a dimple-imprint downstream of boundary-layer trip-wire. *International Journal of Heat and Mass Transfer*, 173 (2021), p. 121242
6. DEPONTE, H., et al., Fluid dynamic investigation of particle-laden suspensions on dimpled surfaces under fouling conditions. *International Journal of Multiphase Flow*, 140 (2021), p. 103651
7. LINKE, B.G., et al., Food additives and their health effects: A review on preservative sodium benzoate. *African Journal of Biotechnology*, 17 (2018) 10, p. 306-310
8. SHAHMOHAMMADI, M., M. JAVADI, M. NASSIRI-ASL, An overview on the effects of sodium benzoate as a preservative in food products. Biotechnology and Health Sciences, 3 (2016) 3, p. 7-11
9. LOCKHART, F., HEAT, Mass Transfer Data Book, *Chemical Engineering Education*,.10 (1976) (4) p. 154-154
10. ROHSENOW, W.M., J.P. HARTNETT, Y.I. CHO, Handbook of heat transfer. McGraw-Hill New York, 3 (1998)
11. VLASOGIANNIS, P., et al., Air–water two-phase flow and heat transfer in a plate heat exchanger. *International Journal of Multiphase Flow*, 28 (2002) 5, p. 757-772
12. KHAN, T., et al., Experimental investigation of single phase convective heat transfer coefficient in a corrugated plate heat exchanger for multiple plate configurations. *Applied Thermal Engineering*, 30 (2010) 8-9, p. 1058-1065
13. MUTHAMIZHI, K., P. KALAICHELVI, Development of Nusselt number correlation using dimensional analysis for plate heat exchanger with a carboxymethyl cellulose solution. Heat and Mass Transfer, 2015. 51(6): p. 815-823
14. LONGO, G., A. GASPARELLA, Refrigerant R134a vaporisation heat transfer and pressure drop inside a small brazed plate heat exchanger. *International journal of refrigeration*,. 30 (2007) 5, p. 821-830
15. GHERASIM, I., et al., Heat transfer and fluid flow in a plate heat exchanger part I. Experimental investigation. *International Journal of Thermal Sciences,* 50 (2011) 8, p. 1492-1498

16.SOMAN, D.P., et al., Experimental study of turbulent forced convection heat transfer and friction factor in dimpled plate heat exchanger. *Applied Thermal Engineering*,. 162 (2019) p. 114254

17. KWON, Y., et al., Heat transfer and pressure drop characteristics of nanofluids in a plate heat exchanger. *Journal of nanoscience and nanotechnology,* 11 (2011) 7, p. 5769-5774

18.CIEŚLIŃSKI, J.T., et al. Performance of a plate heat exchanger operated with water-Al_2O_3 nanofluid. in Applied Mechanics and Materials, *Trans Tech Publ*, 2016

19.GIRAM, D.R., A. PATIL, Experimental and theoretical analysis of heat transfer augmentation from dimpled surface. *International Journal of Engineering Research and Applications*, 3 (2013) 5, p. 19-23